Summer phyto- and bacterioplankton communities during low and high productivity scenarios in the Western Antarctic Peninsula

As Published: https://doi.org/10.1007/s00300-018-2411-5

Publisher: Springer Berlin Heidelberg

Persistent URL: https://hdl.handle.net/1721.1/131555

Version: Author's final manuscript: final author's manuscript post peer review, without publisher's formatting or copy editing

Summer phyto- and bacterioplankton communities during low and high productivity scenarios in the Western Antarctic Peninsula

Sebastián Fuentes[1,2], José Ignacio Arroyo[1,2], Susana Rodríguez-Marconi[3,4], Italo Masotti[3], Tomás Alarcón-Schumacher[1,2], Martin F Polz[5], Nicole Trefault[6], Rodrigo De la Iglesia[1], Beatriz Díez[1,2,7]

[1]Departament of Molecular Genetics and Microbiology, Faculty of Biological Sciences, Pontificia Universidad Católica de Chile, Santiago, Chile; [2]Center for Climate and Resilience Research (CR)2, Santiago, Chile; [3]Facultad de Ciencias del Mar y de Recursos Naturales, Universidad de Valparaíso, Viña del Mar, Chile; [4]Programa de Magister en Oceanografía, Universidad de Valparaíso - Pontificia Universidad Católica de Valparaíso; [5]Department of Civil and Environmental Engineering, Massachusetts Institute of Technology, Cambridge, MA, USA; [6]Center for Genomics and Bioinformatics, Faculty of Sciences, Universidad Mayor, Santiago, Chile; [7]Corresponding author: bdiez@bio.puc.cl, +56223542661

ABSTRACT

Phytoplankton blooms taking place during the warm season drive high productivity in Antarctic coastal seawaters. Important temporal and spatial variations exist in productivity patterns, indicating local constraints influencing the phototrophic community. Surface water in Chile Bay (Greenwich Island, South Shetlands) is influenced by freshwater from the melting of sea ice and surrounding glaciers, however it is not a widely studied system. The phyto- and bacterioplankton communities in Chile Bay were studied over two consecutive summers; during a low productivity period (Chlorophyll *a* < 0.05 mg m^{-3}) and an ascendant phototrophic bloom (Chlorophyll *a* up to 2.38 mg m^{-3}). Microbial communities were analyzed by 16S rRNA – including plastidial – gene sequencing. Diatoms (mainly Thalassiosirales) were the most abundant phytoplankton, particularly during the ascendant bloom. Bacterioplankton in the low productivity period was less diverse and dominated by a few operational taxonomic units (OTUs), related to *Colwellia* and *Pseudoalteromonas*. Alpha diversity was higher during the bloom, where several Bacteroidetes taxa absent in the low productivity period were present. Network analysis indicated that phytoplankton relative abundance was correlated with bacterioplankton phylogenetic diversity and the abundance of several bacterial taxa. Hubs – the most connected OTUs in the network – were not the most abundant OTUs and included some poorly described taxa in Antarctica, such as *Neptunomonas* and *Ekhidna*. In summary, the results of this study indicate that in Antarctic Peninsula coastal waters, such as Chile Bay, higher bacterioplankton community diversity occurs during a phototrophic bloom. This is likely a result of primary production, providing a source of fresh organic matter to bacterioplankton.

Keywords

Bacterioplankton / Phytoplankton / Antarctic Peninsula / 16S rRNA gene sequencing

INTRODUCTION

Increase in temperature and solar radiation during the Antarctic spring/summer causes in ice melt, subsequently triggering cascading effects through marine ecosystems. Micro- and macronutrients are abundant in the Western Antarctic Peninsula (WAP) coastal seawaters, where phytoplankton is mainly influenced by water column mixing (Vernet et al. 2008). During the warm season, mixing varies according to freshwater inputs from glaciers and sea ice, which influence light penetration, salinity and column stratification (Vernet et al. 2008; Gonçalves-Araujo et al. 2015). Phytoplankton blooms during this period are triggered by increased light exposure, temperature and freshwater input (Ducklow et al. 2013). Phytoplankton assimilates inorganic nutrients and releases organic carbon, nitrogen and phosphorous into the water column, generating ideal conditions for mixo- and heterotrophic bacterial growth, as well as eukaryotic grazing. This leads to an overall increase in productivity (Borges Mendes et al. 2012; Cavicchioli 2015). Phototrophic blooms vary, and may be dominated by picophytoplankton, such as prasinophytes (Prézelin et al. 2000; Garibotti et al. 2005); nanophytoplankton, such as haptophytes and cryptophytes; or small diatoms (Garibotti et al. 2005; Egas et al. 2017). Alternatively, microphytoplankton may dominate, including large diatoms and dinoflagellates (Piquet et al. 2008; Gonçalves-Araujo et al. 2015).

In Antarctica, phytoplankton-associated bacterioplankton includes several well-known ubiquitous marine lineages (Buchan et al. 2014), where copiotrophic Flavobacteriales, Alteromonadales, and Rhodobacterales are commonly observed during the warm season (West et al. 2008; Wilkins et al. 2013). In winter, some taxa present low abundances (i.e. rare), however abundance increases during the warm season (Wilkins et al. 2013; Luria et al. 2016). Conversely, reverse dynamics are present in some Gammaproteobacteria, Pelagibacterales and the nitrite-oxidizing *Nitrospina*, with higher abundance during winter (Ghiglione and Murray 2012; Luria et al. 2016). Hence, different seasonal dynamics exist for Antarctic bacterioplankton, ultimately depending on the specific lifestyle of different bacteria.

In addition to seasonal dynamics, year-to-year and short-term variations exist for both phyto- and bacterioplankton (Schloss et al. 2012; Egas et al. 2017). Moreover, local non-predictable factors, such as drifting icebergs can also influence water mixing and subsequently planktonic communities (Dinasquet et al. 2017).

An objective of the Scientific Committee on Antarctic Research (SCAR) is to investigate changes in biological processes at molecular, physiological, population and ecosystem levels (Gutt et al. 2012). Therefore, additional data is required from a variety of Antarctic ecosystems. Chile Bay, located in Greenwich Island (South Shetlands), is a shallow and relatively closed marine system. Recently, this system was described in a study

concerning the feeding regime of spiny plunderfish larvae; results indicated that diatoms, particularly *Thalassiosira* and *Pseudo-nitzschia* species, largely dominate phytoplankton communities (Landaeta et al. 2017). However, there is no available data on bacterioplankton communities, or the relationship between phytoplankton and environmental conditions. Thus, the present study aims to identify the bacterioplankton members associated with these two main diatom groups. For this, we investigated phyto- and bacterioplankton dynamics under different productivity scenarios during two short-term summer sampling periods (2013 and 2014), in Chile Bay.

MATERIALS AND METHODS

Sampling and environmental data

Seawater samples were collected during 2013 and 2014 summer periods at Chile Bay, located on Greenwich Island, South Shetlands (-62.6166, -59.8333, **Fig 1**). Samples from 2013 were collected between January 28th and February 14th; whereas samples from 2014 were collected between February 9th and March 3rd. Subsurface seawater (3 m depth) was pumped up through a 200-µm net to exclude large organisms. For microbial community analyses, 2–3 L of seawater were sequentially filtered through 20-µm, 8-µm and 0.2-µm filters (Sterivex, Merck-Millipore) at the time of sampling. Filters were shipped from Antarctica in liquid nitrogen and further stored at -80°C until DNA extraction to avoid any change in community due to handling. Same procedure was used for both sampling campaigns. By this approach we obtained and analyzed a total of 46 samples, 26 from summer 2013 and 20 from summer 2014 at two size fractions: “small” (0.2–8 µm) and “large” (8–20 µm). We sampled the subsurface water at 3 m depth because Chile Bay is a shallow bay (100 m maximum depth). Light penetration is about 3-7 m (measured with Secchi disc), so we were sure to sample the layer where the light is intensive enough for phototrophs. Meteorological data were obtained from the Chilean Navy station Arturo Prat, located at Chile Bay coast. Precipitation was registered every 3 hours with a 5.4000.00.000 Rain gauge pluviometer (THIES CLIMA, Germany). Wind conditions (direction and intensity) and air temperature were recorded using the Wind Set WA15 anemometer (Vaisala, Finland) and the HMP45D probe (Vaisala, Finland), respectively. Water temperature was measured in a daily basis close to the shore (1–2 m depth) at the vicinity of the station using a temperature sensor QMT110 (Vaisala, Finland) and during sampling

with a multi-parameter sensor (OAKTON PCD650, USA). The environmental variables (wind, precipitation, air and water temperature) were analyzed between January 15th and March 15th, in order to span at least 15 days before and after each sampling period. For paired comparisons between 2013 and 2014 environmental conditions we first assessed normality by the Shapiro-Wilk test, and differences between 2013 and 2014 environmental conditions were estimated by comparing daily mean values using one-way ANOVA (normal distribution) or Kruskal-Wallis (no normal distribution) paired tests.

Chlorophyll *a* (Chl-*a*) and nutrients determination

Seawater was collected by pumping through a 200-µm net in order to exclude large organisms. Seawater (1 L) was filtered through a 0.2-µm filter (Sterivex, Merck-Millipore) which was stored at -80°C until Chl-*a* extraction. Total Chl-*a* was quantified either by methanol or acetone extraction and spectrophotometric or fluorometric determinations, respectively. For the spectrophotometric method, each filter was cut into small pieces and mixed by vortexing with hot methanol (65 ºC). The mix was dark incubated for 5 min at 65 °C and 16 h at room temperature. After the incubation, tubes were centrifuged at maximum speed for 15 min to sediment the disrupted filter pieces. One mL of the supernatant was spectrophotometrically measured at 665 and 750 nm. Eight microliters of HCl 1 M were added, incubated for 1 min and measured again at 665 and 750 nm. To determinate Chl-*a* content, the equation described by Chorus and Bartram (1999) was used with the constant value of 29.62. For the fluorometric method, each filter was cut into small pieces, mixed with acetone 90% v v^{-1} and incubated for 20 h at -20 °C in the dark. After the incubation, 1 mL of the supernatant was measured in a fluorometer ($\lambda_{excitation}$ = 436 nm, $\lambda_{emission}$ = 680 nm). Eight microliters of HCl 1 M were added, incubated for 1 min and measured again at the same excitation and emission wavelengths. For Chl-*a* content calculations, the equation described by Strickland and Parsons (1972) was used. A subset of samples analyzed by both methods yielded comparable results and thus discarded methodology biases.

Seawater for nitrate, nitrite, phosphate and silicic acid determination were collected in triplicate 15 mL polyethylene flasks during sampling. Samples were frozen and stored at -20 °C in the dark until 4–12 hours before analysis, time at which they were thawed at room temperature. Then, nitrate, nitrite, phosphate, and silicate concentrations were measured immediately by pumping through a Technicon AutoAnalyzer® (AA3 Seal Analytical).

DNA extraction, 16S rRNA gene amplification and sequencing

DNA extraction was based on the method described by Díez et al. (2001), with modifications. Briefly, filters were resuspended in lysis buffer (10 mM Tris-HCl pH=8.0, 1 mM EDTA, 0.15 M NaCl, 1% sodium dodecyl sulphate, 0.1 mg ml^{-1} Proteinase K) and sterile glass beads. The mix was incubated at 37 °C for 1 h with vortex mixing every 15 min. NaCl and cetrimonium bromide was added to reach a final concentration of 0.6 M and 1%, respectively, and the mix was incubated at 65 ºC for 10 min. DNA was extracted with phenol-chloroform-isoamyl alcohol (25:24:1) and the residual phenol was eliminated with chloroform-isoamyl alcohol (24:1). The extract was cleaned up by two successive precipitations with cold isopropanol and 70% ethanol. Nucleic acids were quantified using the Qubit DNA probe (Invitrogen); quality was assessed by spectrophotometry (A_{260} A_{280}^{-1} ratio) and integrity by standard agarose gel electrophoresis. The V4 region of the 16S rRNA gene was amplified using the primers PE_16S_V4_515F (ACACGACGCTCTTCCGATCTYRYRGTGCCAGCMGCCGCGGTAA) and PE_16S_V4_786R (CGGCATTCCTGCTGAACCGCTCTTCCGATCTGGACTACHVGGGTWTCTAAT), according to Preheim et al. (2013). Sequencing was conducted on a MiSeq Illumina sequencer at the BioMicro Center, Massachusetts Institute of Technology (Cambridge, MA, USA).

Analysis of the 16S rRNA sequence datasets

Sequence analyses were performed with QIIME v.1.9.1 (Caporaso et al. 2010). First, forward and reverse sequences in raw datasets were assembled and adapters were removed; after which the 99.92% of the reads were 250 nt length and the remaining 0.08% was 230–240 nt length. Sequences were demultiplexed into the 46 samples and grouped into 97% identity Operational Taxonomic Units (OTU) with uclust (Edgar 2010) using the open-reference OTU-picking strategy (Rideout et al. 2014). Mitochondria and unassigned reads, as well as singletons and doubletons, were removed from the OTU table before subsequent analyses. The resulting OTU table that contain the OTUs corresponding to both chloroplast (i.e. as a proxy of photosynthetic eukaryotes) and bacterial communities, was split into two: (1) OTU table with the chloroplast reads in order to analyze phytoplankton community, where the PhytoREF database (Decelle et al. 2015) was used for the taxonomic assignments of chloroplasts. (2) OTU table with bacterial sequences in order to analyze bacterioplankton community, where the SILVA123 database (Quast et al. 2013) was used as a reference for taxonomic assignments. To make comparable bacterioplankton communities, samples were rarefied to 2,901 sequences. Because of this, only 44 samples were analyzed since 2 samples from 2014 (Feb-28 21:30 and Mar-01 13:00) had a sequencing depth of bacterioplankton reads lower than 2,901. Alpha-diversity, richness and Faith's phylogenetic diversity (Faith 1992), metrics were calculated and mean values were compared using two-sample

t-student test. Sequences were submitted to the NCBI BioProject database with the project identification number PRJNA397228, sample accession numbers SAMN07452497 to SAMN07452540.

Network reconstruction

The starting non-rarified OTU table containing both chloroplast and bacterial OTUs was rarified at 2,820 reads sample^{-1}. OTUs present in < 10 samples or present in < 0.001% of total reads were removed prior to network reconstruction. We used a probabilistic graphical model (PGM) approach where the network is reconstructed using the maximum entropy strategy implemented in the R package 'huge' (High-Dimensional Undirected Graph Estimation; Zhao et al. 2012). Briefly, the networks were constructed with the inverse matrix of covariances, where all nonzero elements imply the presence of a link and a zero element is the absence of a link. We used the *glasso* algorithm to estimate the inverse matrix of covariances and the *ric* search criterion to estimate the most stable matrix. For the network of high-level taxonomic groups, OTUs were collapsed to the corresponding level and the taxon abundance was used for PGM. We included the Faith's bacterioplankton phylogenetic diversity (Faith 1992), the relative abundance of chloroplast reads and the relative abundance of bacterial reads. The weight of the links was calculated as the absolute value of the partial correlations among variables. For the four independent networks, the following network properties were calculated in Cytoscape software (Shannon et al. 2003): edge-to-node ratio (E-N; the average numbers of edges per node), clustering coefficient (Clu; ratio of existing links connecting a node's neighbors to each other to the maximum possible number of such links), average number of neighbors (Ann), density (Den; ratio of number of edges to the possible number of edges), connected components (Com; number of subnetworks) and heterogeneity (Het; coefficient of variation of the connectivity distribution). Modularity (Mod; a measure to quantify the extent of how much groups of nodes are more connected among them than with other parts of the network) was estimated in R using the walktrap community finding algorithm (Pons and Latapy 2006).

RESULTS

Environmental features in Chile Bay

Sampling of Chile Bay seawater took place over an 18-day period in summer 2013, and during a 23-day

period in summer 2014. In summer 2014 precipitation was ca. 4-fold higher (Kruskal-Wallis test, $H_1 = 25.1$, $p < 0.0001$), whereas air and water temperature were 1.0 °C lower (Kruskal-Wallis test, $H_1 = 14.3$, $p = 0.0002$) and 1.2 °C lower (Kruskal-Wallis test, $H_1 = 39.3$, $p < 0.0001$), respectively (**Online Resource 1**). Concordant with this difference, water temperature registered during sampling was 0.2 °C lower during the 2014 sampling period (ANOVA, $F_{1,17} = 5.7$, $p = 0.02$). During 2013 there were less frequent and less intense (Kruskal-Wallis test, $H_1 = 13.95$, $p < 0.0001$) wind gusts with a prevalent S-SW wind direction. Conversely in 2014 wind intensity was higher and predominantly N-NE (**Online Resource 1**). Nutrient levels remained stable in Chile Bay throughout both sampling periods. Nitrite (NO_2^-) was 0.29 ± 0.05 µM, n = 6, and 0.18 ± 0.02 µM, n = 16, in 2013 and 2014, respectively. Nitrate (NO_3^-) was 24.9 ± 3.3 µM, n = 7, and 22.9 ± 2.6 µM, n = 16, in 2013 and 2014, respectively. Silicate (SiO_3^{-2}) was 42.2 ± 8.1 µM, n = 7, and 48.0 ± 5.0 µM, n = 16, in 2013 and 2014, respectively. Phosphate (PO_4^{-3}) was 1.8 ± 0.2 µM, n = 7 and n = 13, both years.

Phytoplankton communities

A total of 46 samples were collected over both sampling periods; 26 from summer 2013 (14 small and 12 large size fractions) and 20 from summer 2014 (11 small and 9 large size fractions). Hereafter, samples groups are referred as “2013-small”, “2013-large”, “2014-small” and “2014-large”. The chlorophyll *a* (Chl-*a*) content was lower during the sampled period in 2013 (< 0.05 mg m^{-3}), with respect to 2014, where an increasing pattern was observed, from 0.2 to 2.38 mg m^{-3} (**Fig 2a** and **2b**, lines). Microbial communities were analyzed by sequencing the V4 region from the 16S rRNA gene, enabling the analysis of both bacteria and chloroplasts from phototrophic eukaryotes. Chloroplast read percentages were 0.2 ± 0.1, n = 14, and 0.8 ± 0.7, n = 12, in samples from 2013-small 2013-large, respectively (**Fig 2a**, bars). In 2014-small and 2014-large, chloroplast reads represented 6.0 ± 5.7, n = 11, and 57.8 ± 26.4, n = 9, respectively (**Fig 2b**, bars). Sequences were grouped into 97% identity OTUs and the taxonomy was further assessed for the two years and cell size fractions. Ochrophyta was the dominant phylum over the four groups, with the following percentages; 53.7 ± 18.2, n = 13, in 2013-small; 73.2 ± 16.0, n = 12, in 2013-large; 62.6 ± 17.5, n = 11, in 2014-small; 88.6 ± 8.8, n = 9, in 2014-large (summarized in **Fig 2c**). Haptophyta was the second most abundant phytoplankton phyla, with the following percentages; 30.1 ± 13.4, n = 13, in 2013-small; 18.6 ± 15.3, n = 12, in 2013-large; 25.7 ± 10.8, n = 11, in 2014-small; 8.1 ± 5.4, n = 9, in 2014-large. Following, Cryptophyta had the third highest abundance, with the following percentages; 11.4 ± 14.1, n = 13, in 2013-small; 1.9 ± 2.4, n = 12, in 2013-large; 10.0 ± 9.5, n = 11, in 2014-small; 2.8 ± 3.5, n = 9, in 2014-large. Chlorophyta represented approximately 5% of chloroplast reads in both of the 2013 sample groups, and

less than 1% during 2014. Other phyla such as Streptophyta and Rhodophyta represented less than 0.5% over all the four groups. Diatoms (Bacillariophyta) were the most abundant Ochrophyta over the four sample groups; specifically Thalassiosirales was the most abundant order in the 2014-large group (**Fig 2c**). Other Ochrophyta, such as Pelagomonadales and Florenciellales, were present in lower abundances, between approximately 1% and 14% across the four sample groups. Two orders of the phylum Haptophyta, Prymnesiales and Phaeocystales, were present. Phaeocystales was the dominating order (23%) the 2014-small group (**Fig 2c**).

Bacterioplankton communities

Subsequently, bacterioplankton from the two periods were investigated. Similar dynamics were observed between bacterial alpha diversity and Chl-*a* levels, with background variation in 2013 (**Fig 3a**) and an increasing trend observed during the 2014 phototrophic bloom (**Fig 3b**). This was confirmed for phylogenetic diversity (**Fig 3b**) and richness (**Online resource 2**). Bacterioplankton communities were ca. 2-fold more diverse in terms of both phylogenetic diversity (Two-sample *t* test, $t_{42} = 9.70$, $p = 0.002$) and richness (Two-sample *t* test, $t_{42} = 8.54$, $p = 0.002$) in 2014 compared to 2013.

The low productivity period (summer 2013) was largely dominated by Proteobacteria (**Fig 3c**). Over half of the bacterial reads in the 2013 samples were from two Alteromonadales genera; *Colwellia* (38.8 ± 15.8 reads percent, n = 14, in 2013-small; 25.7 ± 14.5 reads percent, n = 12, in 2013-large); and *Pseudoalteromonas* (31.9 ± 14.1 reads percent, n = 14, 2013-small; 35.7 ± 15.9 reads percent, n = 12, in 2013-large). The relative abundances of taxa in each year were consistent across samples and not just an average distorted by few samples with high proportion of these taxa (**Online resource 3**). Conversely, during the bloom growth period (summer 2014), the bacterial community was dominated by Bacteroidetes. Flavobacteriia were mostly represented, in reads percent, by *Polaribacter* (8.0 ± 4.9, n = 11, small cell fraction; 6.7 ± 5.4, n = 7, large cell fraction), *Cloacibacterium* (5.1 ± 7.1, n = 11, small cell fraction; 9.1 ± 12.2, n = 7, large cell fraction), *Ulvibacter* (3.1 ± 1.8, n = 11, small cell fraction; 10.9 ± 9.7, n = 7, large cell fraction), NS5 Marine Group (6.5 ± 4.3, n = 11, small cell fraction; 2.7 ± 2.9, n = 7, large cell fraction) and *Maribacter* (2.0 ± 2.3, n = 11, small cell fraction; 4.3 ± 6.5, n = 7, large cell fraction). Cytophagia members included two genera absent during the low productivity period in 2013; *Reichenbachiella* (16.8 ± 13.0, n = 11, small cell fraction; 6.3 ± 5.6, n = 7, large cell fraction) and *Ekhidna* (6.0 ± 5.1, n = 11, small cell fraction; 2.7 ± 5.1, n = 7, large cell fraction). Furthermore, Alteromonadales that dominated in summer 2013 represented less than the 6% across 2014 samples.

Network of phyto- and bacterioplankton communities

Network reconstruction indicated that nodes corresponding to 2014 OTUs were tightly clustered apart from 2013 OTUs (**Fig 4a**). Nodes corresponding to common OTUs (i.e. present both summers) were sparsely located across the network, whereas phytoplankton nodes were present at the center and connecting nodes from both years (**Fig 4a**). Half of the phytoplankton nodes were diatoms (27 of 54, data not shown). The network presents the characteristic structure for ecological networks, with degree frequencies presenting a power-law-like distribution (slope of -0.89 and r-squared of 0.51). The majority of nodes have few connections, but some nodes are highly interconnected, i.e. hubs (**Fig 4b**). The ten most interconnected hubs (i.e. degree > 50) include several lineages belonging to Alpha-, Gamma- and Epsilonproteobacteria, Cytophagia and Flavobacteriia classes (**Fig 4b**). Only six phytoplankton nodes had a degree greater than 30, which were taxonomically affiliated to Diatoms (3 OTUs), Phaeocystales (2 OTUs) and Pelagomonadales (1 OTU). None of the hubs corresponded to Thalassiosirales, but the two most connected phytoplankton hubs (degree = 49) corresponded to a Bacillareaceae and to an unclassified diatom (not shown). An additional network of high-level taxa (i.e. phylum and class) revealed an association between phytoplankton and all major bacterioplankton taxa in the same connected component. Exceptions to this case were Chloroflexi, Tenericutes, SR1 and Chlamidyae phyla, which were present in separate components of the network (**Fig. 4c**).

Further analysis was carried out for the two cell size fractions and sampling periods. The structure of networks revealed that both of the 2013 communities were simpler than the 2014 communities, indicated by the lower values of the edge-to-node ratio (E-N), clustering coefficient (Clu), average number of neighbors (Ann) and density (Den). All these previously mentioned metrics are indicators of the overall network connectivity (**Online resource 4**). Furthermore, the connected components (Com) were higher in 2013 networks, with more components with few nodes and a large proportion of zero degree nodes (excluded from plots).

DISCUSSION

In general, Antarctic microbial communities follow regular seasonal patterns (Cavicchioli 2015). However, environmental conditions present year-to-year and spatial variation (Schloss et al. 2012; Gonçalves-Araujo et al. 2015). Primary productivity (based on Chl-*a* concentration) was investigated over two distinct sampling periods, during the summer seasons of 2013 and 2014, in the coastal marine system of Chile Bay. Low

Chl-*a* concentration during the 2013 summer period was comparable to levels observed in Antarctic open seawaters during summer (Borges Mendes et al. 2012). Conversely, Chl-*a* content reaching 2.38 mg m^{-3} was observed in summer 2014, coinciding with the occurrence of primary producer blooms during summer in Antarctic coastal surface seawaters (Borges Mendes et al. 2012; Schloss et al. 2012; Luria et al. 2016). Diatoms are one of the predominant Antarctic primary producers (Borges Mendes et al. 2012; Gonçalves-Araujo et al. 2015). In the summer of 2014, *Thalassiosira* and several *Pseudo-nitzschia* species were the dominant diatom populations in Chile bay, representing more than 68% and 10% of the phytoplankton community, respectively (Landaeta et al. 2017). The present study aims to identify bacterioplankton associated with these two main phytoplankton groups. Thus, the fractionation size (i.e. 8 µm size cut) was selected to facilitate the study of both solitary and chain-forming *Thalassiosira minuscula* (Thalassiosirales) and *Pseudo-nitzschia* spp. (Bacillariales) in the large fraction separated from the smaller phytoplankton. This threshold size has been used to differentiate small (3 – 8 µm) from large (> 8 µm) particle associated bacterioplankton (Milici et al. 2017), however, in this case it enabled the separation of bacterioplankton into two groups; one associated with the two dominant diatom populations, and the other associated with smaller phytoplankton. The PhytoRef database was used for taxonomic assignation of chloroplast reads because it is updated, curated and dedicated to plastidial 16S rRNA sequences (Decelle et al. 2015). When checking the results, there are no concerns about it because (1) low number of unassigned reads and (2) taxonomy of main groups is consistent with those found by Landaeta et al. (2017) by microscopic cell counts.

As expected, Thalassiosirales were the most abundant diatoms during summer 2014 phytoplankton bloom, particularly within the larger size fraction (**Fig 2c**), where chloroplasts reads percent were the highest, in average 58% (**Fig 2b**, light bars). Although Thalassiosirales were also present in the other three sample groups, they reached their highest proportion in 2014-large (**Fig 2c**). The low proportion of Thalassiosirales present in both small fractions was possibly due to the presence of small Thalassiosirales, such as *T. mendoliana* (< 8 µm), also present in Chile Bay (Landaeta et al. 2017). However, *Thalassiosira* is one of the dominant phytoplankton present during summer in Fildes Bay, King George Island (Egas et al. 2017), supporting the concept that diatoms are one of the main primary producers within the WAP coast.

Remarkably, the increased phylogenetic diversity (**Fig 3b**) and richness (**Online resource 2**) of the bacterioplankton associated with the phytoplankton bloom, is consistent with the “species energy” theory, which predicts a linear relationship between richness and available energy, e.g. productivity (Wright 1983). Similarly, the “more individuals” hypothesis suggests that an increase in available energy reduces extinction probability in

populations, leading to increased community richness (Allen et al. 2007). This is consistent with the results from this study, as well as with other reports of seawater from Adelaide Island (WAP), where a rapid shift in Bacteroidetes population occurred after phytoplankton blooms (Piquet et al. 2011). Bacterioidetes was the dominant phyla during the ascendant bloom period. Most Bacteroidetes have a preference for a particle-attached lifestyle and degradation of high-molecular-weight compounds (Fernández-Gómez et al. 2013), thus, this is compatible with the increased proportion in the 2014 community. Some genera, such as *Polaribacter*, *Ulvibacter* and *Maribacter* (Flavobacteriales) were present during this period. *Ulvibacter* and *Maribacter* have been associated with green algae such as *Ulva lactuca* and *Pyramimonas gelidicola*, both Chlorophyta (Nedashkovskaya et al. 2004; Zhang et al. 2009). However, these bacterial genera may have interacted with alternative species of phytoplankton (i.e. not Chlorophyta) due to the low proportion of Ulvales or Pyramimonadales in chloroplast reads during the 2014 sampling period (**Fig 2c**). *Polaribacter* and *Ulvibacter* have been described in association with spring phytoplankton blooms in the North Sea, where *Ulvibacter* is positively correlated with diatoms and haptophytes (Teeling et al. 2016). Thus, the higher proportion of *Ulvibacter* in summer 2014 could be due to diatoms. In the present study, *Reichenbachiella* was also abundant during the ascendant diatom bloom. *Reichenbachiella* may become abundant in response to chitin amendments in Antarctic and Patagonian seawaters (Wietz et al. 2015), and have been found predominantly associated with large particles (i.e. >8 µm) in the Southern Ocean (Milici et al. 2017). Chitin is one of the most abundant marine polymers, as it is found in crustacean exoskeletons, zooplankton, and diatoms (Durkin et al. 2009). Therefore, during the bloom period *Reichenbachiella* spp. could be actively recycling this polymer in Chile Bay.

In summer 2013, the bacterioplankton community was largely dominated by Alteromonadales (**Fig 3c**). A similar bacterial composition was observed next to the Dotson Ice Shelf, West Antarctica. Here, Colwelliaceae dominated following organic amendments in low Chl-*a,* deep waters, whereas other taxa, such as *Pseudoalteromonas*, Oceanospirillales and *Polaribacter*, responded to a lesser extent (Dinasquet et al. 2017). Both Colwelliaceae and Alteromonadaceae rapidly increase in cell number after organic matter enrichment (Allers et al. 2008). For instance, the metabolic versatility of Colwelliaceae allows rapidly responding and adapting to environmental changes, as shown by the metatranscriptomic analysis of seawater incubations in experimental bioreactors (Stewart et al. 2012). In the present study, the dominance of both taxa was consistently found throughout the 2013 sampling period (**Online resource 3**). This discards possible bottle effect such as that described by Stewart et al. (2013), which could artificially distort the proportion of fast-growing taxa. Both *Collwellia* and *Pseudoalteromonas* have been associated with decaying *Phaeocystis antarctica* (Haptophyta)

blooms, where they recycle the organic matter from senescent *Phaeocystis* cells prior to sedimentation (Delmont et al. 2014). Although Phaeocystales were present in the 2013 summer sampling period, chloroplast reads and Chl-*a* levels were low enough to disregard the occurrence of a bloom during the period (**Fig 2a**). Thus, the sampling period in summer 2013 may coincide with a *Phaeocystis* post-bloom scenario, potentially related to the overrepresentation of *Collwellia* and *Pseudoalteromonas*. Furthermore, some *Pseudoalteromonas* spp. produce algicidal agents (Lovejoy et al. 1998) likely to be involved in phototrophic community regulation and the decline of planktonic community blooms (Amaro et al. 2005). However, the present study could not establish if Alteromonadales dominance caused a poor or delayed phototrophic bloom, or vice versa. Ideally, future studies will require controlled experimental setups to assess the dynamic phyto- and bacterioplankton community interactions.

The analysis of the entire community was performed by network reconstruction. This approach assesses all possible interactions within a community, referred as the co-variation of the abundance of one population with another. This includes, but is not limited to, metabolite interchange, niche overlap and resource competition (Barberán et al. 2012; Bar-Massada 2015). Phytoplankton nodes were linked not only with bacterioplankton nodes from the bloom period, but also for the 2013 OTUs (**Fig 4a**). A closer interaction of the community during the ascendant bloom period is indicated by tighter and more connected module of summer 2014 nodes. This suggests that the co-occurrence of certain bacterial populations is likely to be due to using similar phytoplankton-derived organic compounds or, at least, derived from similar phytoplankton populations (Riemann et al. 2000; Buchan et al. 2014). This is supported by the four independent networks (**Online resource 4**), in which the 2014-large network is a single highly-interconnected network where every node (i.e. OTU) is connected with at least one another node in the network. On the other hand, the less connected 2013 community module (**Fig 4a**), and the structure of the two 2013 size fractions networks (**Online resource 4**), suggest that during this summer period with low primary production, bacteria are probably metabolizing alternative organic compounds that are not derived from phytoplankton. For instance, under low Chl-*a* conditions, such as the Arctic winter, a higher number of substrates are used by the bacterioplankton compared to spring, when phytoplankton blooms provide fresh organic sources (Sala et al. 2008). The several unconnected sub-networks along with the high proportion zero degree nodes observed in summer 2013 supports the idea that most community members use a variety of metabolic strategies to withstand the absence of a phytoplankton blooms in Antarctic waters.

Half of the phytoplankton nodes in the network (**Fig 4a**) corresponded to diatoms, highlighting the significance of these phototrophs in Antarctic coastal seawater. However, none of the phytoplankton hubs

corresponded to Thalassiosirales, the dominant diatom in Chile Bay during summer 2014 (Landaeta et al. 2017 and **Fig 2c**). One of the two most connected phytoplankton hubs corresponded to Bacillareaceae and potentially corresponded to any of the *Pseudo-nitzschia* species, which was the second diatom in abundance after *Thalasiossira* (Landaeta et al. 2017). *Pseudo-nitzschia* and *Phaeocystis* species are ubiquitous in Antarctic coastal seawaters (DiTullio et al. 2000; Almandoz et al. 2008). The results from this study reinforce the concept that the most abundant members may not be the most important within the community, e.g. keystone species are not abundant by definition (Power et al. 1996). Similarly, out of the most abundant Bacterioplankton species, for instance, *Colwellia* and *Pseudoalteromonas,* none were observed in the hubs during summer 2013 (**Fig 4b**). In turn, the most connected node corresponded to the genus *Neptunomonas*, which includes members from marine sediments, as well as epiphytic bacteria from red algae *Pyropia yezoensis* (Rhodophyta) and polycyclic aromatic hydrocarbons degrader (Handayani et al. 2014). Information regarding their ecological role in Antarctic seawaters is not seemingly available. Conversely, the role of the two hubs corresponding to *Reichenbachiella* may be related to the degradation of diatom chitin (Wietz et al. 2015), as previously mentioned. Despite being present in low numbers, a node corresponding to *Ekhidna* was observed to be a hub. This poorly characterized Bacteroidetes genus has only one described species, isolated from oligotrophic waters in the South East Pacific Gyre (Alain et al. 2010). Since no additional information regarding this genus is available, its ecological role in Antarctic environments remains undetermined.

Considering the proportion of Chl-*a* values and chloroplast reads, it may be considered that 2013 and 2014 summer samples were taken at different stages of phytoplankton blooms. It is likely that the summer 2013 samples were taken during a *Phaeocystis* post-bloom stage, whereas the summer 2014 samples were taken during an increasing diatom bloom. Thus, the present study may be considered as snapshots from two contrasting scenarios in seawater during the summer season, where the structure and composition of different bacterioplankton communities depends on phytoplankton influence. Likely due to organic matter input from the phytoplankton blooms, indicated by an increase in the community alpha diversity, and the relative complexity of the bacterioplankton as well as the entire microbial community. These results agree with previous studies carried out in other Antarctic locations. Finally, this study is the first report of bacterioplankton communities from Chile Bay and describes the relevance of poorly described bacterioplankton members. Future work will require the generation of further annual datasets in order to fully characterize bacterioplankton dynamics and activities in this specific Antarctic coastal marine ecosystem.

ACKNOWLEDGEMENTS

The authors gratefully acknowledge to the Armada de Chile staff at Arturo Prat Station and the staff from the Chilean Antarctic Institute (INACH); their support made possible the sampling in Chile Bay. We also thank the Department of Climatology, Centro Meteorológico de Valparaíso, Armada de Chile, for the meteorological data. Thanks to María Estrella Alcamán, Cynthia Sanhueza, Laura Farías and Josefa Verdugo for their assistance with sample collection.

This work was financially supported by the grants INACH15-10, INACH_RG_09_17, CONICYT for international cooperation DPI20140044, FONDAP N°15110009, FONDECYT postdoctoral N°3160424, CONICYT PhD scholarship N°21130515 and CONICYT magister scholarship N°22172113.

COMPLIANCE WITH ETHICAL STANDARDS

The authors declare that they have no conflict of interest. This article does not contain any studies with human participants or animals performed by any of the authors.

REFERENCES

Alain K, Tindall BJ, Catala P, et al (2010) *Ekhidna lutea* gen. nov., sp. nov., a member of the phylum Bacteroidetes isolated from the South East Pacific Ocean. Int J Syst Evol Microbiol 60:2972–2978. https://doi.org/10.1099/ijs.0.018804-0

Allen A, Gillooly J, Brown J (2007) Recasting the species-energy hypothesis: the different roles of kinetic and potential energy in regulating biodiversity. In: Storch D, Marquet P, Brown J (eds) Scaling biodiversity. Cambridge University Press, pp 283–299

Allers E, Niesner C, Wild C, Pernthaler J (2008) Microbes enriched in seawater after addition of coral mucus. Appl Environ Microbiol 74:3274–3278. doi: 10.1128/AEM.01870-07

Almandoz GO, Ferreyra GA, Schloss IR, et al (2008) Distribution and ecology of *Pseudo-nitzschia* species

(Bacillariophyceae) in surface waters of the Weddell Sea (Antarctica). Polar Biol 31:429–442. https://doi.org/10.1007/s00300-007-0369-9

Amaro AM, Fuentes MS, Ogalde SR, et al (2005) Identification and characterization of potentially algal-lytic marine bacteria strongly associated with the toxic dinoflagellate *Alexandrium catenella*. J Eukaryot Microbiol 52:191–200. https://doi.org/10.1111/j.1550-7408.2005.00031.x

Bar-Massada A (2015) Complex relationships between species niches and environmental heterogeneity affect species co-occurrence patterns in modelled and real communities. Proc R Soc Biol Sci 282:20150927. https://doi.org/10.1098/rspb.2015.0927

Barberán A, Bates ST, Casamayor EO, Fierer N (2012) Using network analysis to explore co-occurrence patterns in soil microbial communities. ISME J 6:343–351. https://doi.org/10.1038/ismej.2011.119

Borges Mendes CR, Silva de Souza M, Tavano Garcia VM, et al (2012) Dynamics of phytoplankton communities during late summer around the tip of the Antarctic Peninsula. Deep Res Part I Oceanogr Res Pap 65:1–14. https://doi.org/10.1016/j.dsr.2012.03.002

Buchan A, LeCleir GR, Gulvik CA, Gonzalez JM (2014) Master recyclers: features and functions of bacteria associated with phytoplankton blooms. Nat Rev Microbiol 12:686–698. https://doi.org/10.1038/nrmicro3326

Caporaso JG, Kuczynski J, Stombaugh J, et al (2010) QIIME allows analysis of high-throughput community sequencing data. Nat Methods 7:335–336. https://doi.org/10.1038/NMETH.F.303

Cavicchioli R (2015) Microbial ecology of Antarctic aquatic systems. Nat Rev Microbiol 13:691–706. https://doi.org/10.1038/nrmicro3549

Chorus I, Bartram J (1999) Toxic cyanobacteria in water. A guide to their public health consequences, monitoring and management. World Health Organization

Decelle J, Romac S, Stern RF, et al (2015) PhytoREF: a reference database of the plastidial 16S rRNA gene of photosynthetic eukaryotes with curated taxonomy. Mol Ecol Resour 15:1435–1445. https://doi.org/10.1111/1755-0998.12401

Delmont TO, Hammar KM, Ducklow HW, et al (2014) *Phaeocystis antarctica* blooms strongly influence bacterial community structures in the Amundsen Sea polynya. Front Microbiol 5:1–13. https://doi.org/10.3389/fmicb.2014.00646

Díez B, Pedrós-Alió C, Massana R (2001) Study of genetic diversity of eukaryotic picoplankton in different oceanic regions by small-subunit rRNA gene cloning and sequencing. Appl Environ Microbiol 67:2932–2941. https://doi.org/10.1128/AEM.67.7.2932

Dinasquet J, Richert I, Logares R, et al (2017) Mixing of water masses caused by a drifting iceberg affects bacterial activity, community composition and substrate utilization capability in the Southern Ocean. Environ Microbiol 19:2453–2467. https://doi.org/10.1111/1462-2920.13769

DiTullio GR, Grebmeier JM, Arrigo KR, et al (2000) Rapid and early export of *Phaeocystis antarctica* blooms in the Ross Sea, Antarctica. Nature 404:595–598. https://doi.org/10.1038/35007061

Ducklow H, Fraser W, Meredith M, et al (2013) West Antarctic Peninsula: an ice-dependent coastal marine ecosystem in transition. Oceanography 26:190–203. https://doi.org/10.5670/oceanog.2013.62

Durkin CA, Mock T, Armbrust EV (2009) Chitin in diatoms and its association with the cell wall. Eukaryot Cell 8:1038–1050. https://doi.org/10.1128/EC.00079-09

Edgar RC (2010) Search and clustering orders of magnitude faster than BLAST. Bioinformatics 26:2460–2461. https://doi.org/10.1093/bioinformatics/btq461

Egas C, Henríquez-Castillo C, Delherbe N, et al (2017) Short timescale dynamics of phytoplankton in Fildes Bay, Antarctica. Antarct Sci 29:1–12. https://doi.org/10.1017/S0954102016000699

Faith DP (1992) Conservation evaluation and phylogenetic diversity. Biol Conserv 61:1–10. https://doi.org/10.1016/0006-3207(92)91201-3

Fernández-Gómez B, Richter M, Schuler M, et al (2013) Ecology of marine Bacteroidetes: a comparative genomics approach. ISME J 7:1026–1037. https://doi.org/10.1038/ismej.2012.169

Garibotti IA, Vernet M, Ferrario ME (2005) Annually recurrent phytoplanktonic assemblages during summer in the seasonal ice zone west of the Antarctic Peninsula (Southern Ocean). Deep Res Part I Oceanogr Res Pap 52:1823–1841. https://doi.org/10.1016/j.dsr.2005.05.003

Ghiglione J-F, Murray AE (2012) Pronounced summer to winter differences and higher wintertime richness in coastal Antarctic marine bacterioplankton. Environ Microbiol 14:617–629. https://doi.org/10.1111/j.1462-2920.2011.02601.x

Gonçalves-Araujo R, Silva de Souza M, Tavano VM, Eiras Garcia CA (2015) Influence of oceanographic features on spatial and interannual variability of phytoplankton in the Bransfield Strait, Antarctica. J Mar Syst 142:1–15. https://doi.org/10.1016/j.jmarsys.2014.09.007

Gutt J, Adams B, Bracegirdle T, et al (2012) Antarctic thresholds - Ecosystem resilience and adaptation: a new SCAR-biology programme. Polarforschung 82:147–150. https://doi.org/10.013/epic.42531.d001

Handayani M, Sasaki H, Matsuda R, et al (2014) Characterization of an Epiphytic Bacterium *Neptunomonas* sp . BPy-1 on the Gametophytes of a Red Alga *Pyropia yezoensis*. Am J Plant Sci 5:3652–3661.

https://doi.org/10.4236/ajps.2014.524381

Landaeta MF, Vera-Duarte J, Manríquez K, et al (2017) Trophic plasticity of larval notothenioid fish *Harpagifer antarcticus* in shallow waters from the South Shetland Islands, Antarctica. Polar Biol 40:837–851. https://doi.org/10.1007/s00300-016-2009-8

Lovejoy C, Bowman JP, Hallegraeff GM (1998) Algicidal effects of a novel marine *Pseudoalteromonas* isolate (class Proteobacteria, Gamma subdivision) on harmful algal bloom species of the genera *Chattonella*, *Gymnodinium*, and *Heterosigma*. Appl Environ Microbiol 64:2806–2813.

Luria C, Amaral-Zettler L, Ducklow H, Rich J (2016) Seasonal succession of bacterial communities in coastal waters of the western Antarctic Peninsula. Front Microbiol 7:1731. https://doi.org/10.3389/fmicb.2016.01731

Milici M, Vital M, Tomasch J, et al (2017) Diversity and community composition of particle-associated and free-living bacteria in mesopelagic and bathypelagic Southern Ocean water masses: evidence of dispersal limitation in the Bransfield Strait. Limnol Oceanogr 62:1080–1095. https://doi.org/10.1002/lno.10487

Nedashkovskaya OI, Kim SB, Han SK, et al (2004) *Ulvibacter litoralis* gen. nov., sp. nov., a novel member of the family Flavobacteriaceae isolated from the green alga *Ulva fenestrata*. Int J Syst Evol Microbiol 54:119–123. https://doi.org/10.1099/ijs.0.02757-0

Piquet AMT, Bolhuis H, Davidson AT, et al (2008) Diversity and dynamics of Antarctic marine microbial eukaryotes under manipulated environmental UV radiation. FEMS Microbiol Ecol 66:352–366. https://doi.org/10.1111/j.1574-6941.2008.00588.x

Piquet AMT, Bolhuis H, Meredith MP, Buma AGJ (2011) Shifts in coastal Antarctic marine microbial communities during and after melt water-related surface stratification. FEMS Microbiol Ecol 76:413–427. https://doi.org/10.1111/j.1574-6941.2011.01062.x

Pons P, Latapy M (2006) Computing communities in large networks using random walks. J Graph Algorithms Appl 10:191–218. https://doi.org/10.7155/jgaa.00124

Power ME, Tilman D, Estes JA, et al (1996) Challenges in the Quest for Keystones. Bioscience 46:609–620. https://doi.org/10.2307/1312990

Preheim SP, Perrotta AR, Martin-Platero AM, et al (2013) Distribution-based clustering: using ecology to refine the operational taxonomic unit. Appl Environ Microbiol 79:6593–603. https://doi.org/10.1128/AEM.00342-13

Prézelin BB, Hofmann EE, Mengelt C, John M Klinck (2000) The linkage between Upper Circumpolar DeepWater (UCDW) and phytoplankton assemblages on the west Antarctic Peninsula continental shelf. J

Mar Res 58:165–202. https://doi.org/10.1357/002224000321511133

Quast C, Pruesse E, Yilmaz P, et al (2013) The SILVA ribosomal RNA gene database project: improved data processing and web-based tools. Nucleic Acids Res 41:590–596. https://doi.org/10.1093/nar/gks1219

Rideout JR, He Y, Navas-Molina JA, et al (2014) Subsampled open-reference clustering creates consistent, comprehensive OTU definitions and scales to billions of sequences. PeerJ 2:e545. https://doi.org/10.7717/peerj.545

Riemann L, Steward GF, Azam F (2000) Dynamics of bacterial community composition and activity during a mesocosm diatom bloom. Appl Environmantal Microbiol 66:578–587. https://doi.org/10.1128/AEM.66.2.578-587.2000

Sala MM, Terrado R, Lovejoy C, et al (2008) Metabolic diversity of heterotrophic bacterioplankton over winter and spring in the coastal Arctic Ocean. Environ Microbiol 10:942–949. https://doi.org/10.1111/j.1462-2920.2007.01513.x

Schloss IR, Abele D, Moreau S, et al (2012) Response of phytoplankton dynamics to 19-year (1991-2009) climate trends in Potter Cove (Antarctica). J Mar Syst 92:53–66. https://doi.org/10.1016/j.jmarsys.2011.10.006

Shannon P, Markiel A, Ozier O, et al (2003) Cytoscape: a software environment for integrated models of biomolecular interaction networks. Genome Res 13:2498–2504. https://doi.org/10.1101/gr.1239303

Stewart FJ, Dalsgaard T, Young CR, et al (2012) Experimental incubations elicit profound changes in community transcription in OMZ bacterioplankton. PLoS One. doi: 10.1371/journal.pone.0037118

Strickland JDH, Parsons TR (1972) A practical handbook of seawater analysis, 2nd edn. The Alger Press Ltd.

Teeling H, Fuchs BM, Bennke CM, et al (2016) Recurring patterns in bacterioplankton dynamics during coastal spring algae blooms. Elife 5:e11888. https://doi.org/10.7554/eLife.11888

Vernet M, Martinson D, Iannuzzi R, et al (2008) Primary production within the sea-ice zone west of the Antarctic Peninsula: I - Sea ice, summer mixed layer, and irradiance. Deep Res Part II Top Stud Oceanogr 55:2068–2085. https://doi.org/10.1016/j.dsr2.2008.05.021

West NJ, Obernosterer I, Zemb O, Lebaron P (2008) Major differences of bacterial diversity and activity inside and outside of a natural iron-fertilized phytoplankton bloom in the Southern Ocean. Environ Microbiol 10:738–756. https://doi.org/10.1111/j.1462-2920.2007.01497.x

Wietz M, Wemheuer B, Simon H, et al (2015) Bacterial community dynamics during polysaccharide degradation at contrasting sites in the Southern and Atlantic Oceans. Environ Microbiol 17:3822–3831.

https://doi.org/10.1111/1462-2920.12842

Wilkins D, Yau S, Williams TJ, et al (2013) Key microbial drivers in Antarctic aquatic environments. FEMS Microbiol Rev 37:303–35. https://doi.org/10.1111/1574-6976.12007

Wright DH (1983) Species-energy theory: an extension of species-area theory. Oikos 41:496–506.

Zhang GI, Hwang CY, Kang SH, Cho BC (2009) *Maribacter antarcticus* sp. nov., a psychrophilic bacterium isolated from a culture of the Antarctic green alga *Pyramimonas gelidicola*. Int J Syst Evol Microbiol 59:1455–1459. https://doi.org/10.1099/ijs.0.006056-0

Zhao T, Liu H, Roeder K, et al (2012) The huge package for high-dimensional undirected graph estimation in R. J Mach Learn Res 13:1059–1062.

TABLES AND FIGURES CAPTIONS

Fig. 1 Sampling point in Chile Bay, Greenwich Island, Antarctica. The point indicates the approximate location of the sampled point in the mouth of Chile Bay

Fig. 2 Phytoplankton relative abundance and Chl-*a* concentration during the sampled periods in a) summer 2013 and b) summer 2014. Bars represent the normalized relative abundance (reads percent) in each sample. Two bars are shown for each sampling time, corresponding to the small (0.2 – 8 µm) and large (8 – 20 µm) cell size fractions. Lines correspond to the Chl-*a* levels, where the measured samples are depicted by filled circles. c) Taxonomic assignment of chloroplast reads in each year and fraction size. Charts show the relative abundance of taxa at the order level

Fig. 3 Bacterioplankton phylogenetic diversity dynamics during the sampled periods in a) summer 2013 and b) summer 2014. c) Taxonomic assignment of reads in each year and fraction size. Charts show the relative abundance of taxa at the genus level, where genera <1% abundance were grouped and are shown as “All other taxa”

Fig. 4 Networks of the phyto- and bacterioplankton communities. a) Network of all OTUs with an occupancy >10

and abundance >0.001%. The network shows a module of nodes from summer 2013 on the left and a tight module of nodes from summer 2014 on the right. At the center, phytoplankton nodes are connecting nodes from both summers. Colors indicate the high-level taxonomy of the nodes. b) Degree distribution of nodes. Black points indicate the hubs, this is, the highly connected nodes. The taxonomic affiliation of the top-ten hubs (> 50 connections) is listed and the OTU number is shown in parenthesis. c) Network of high-level taxonomic groups, including the bacterioplankton phylogenetic diversity (Faith PD) and the relative abundance of chloroplast (Eukaryote phytoplankton) and bacterial (Bacterioplankton) reads. The width of the link represents the extent of the absolute value of the partial correlations among variables, i.e. the weight of the link

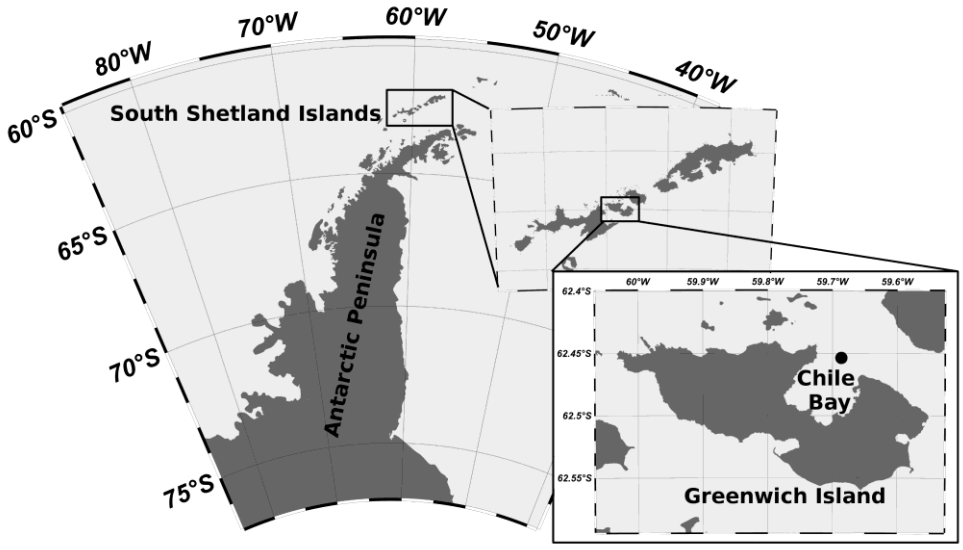

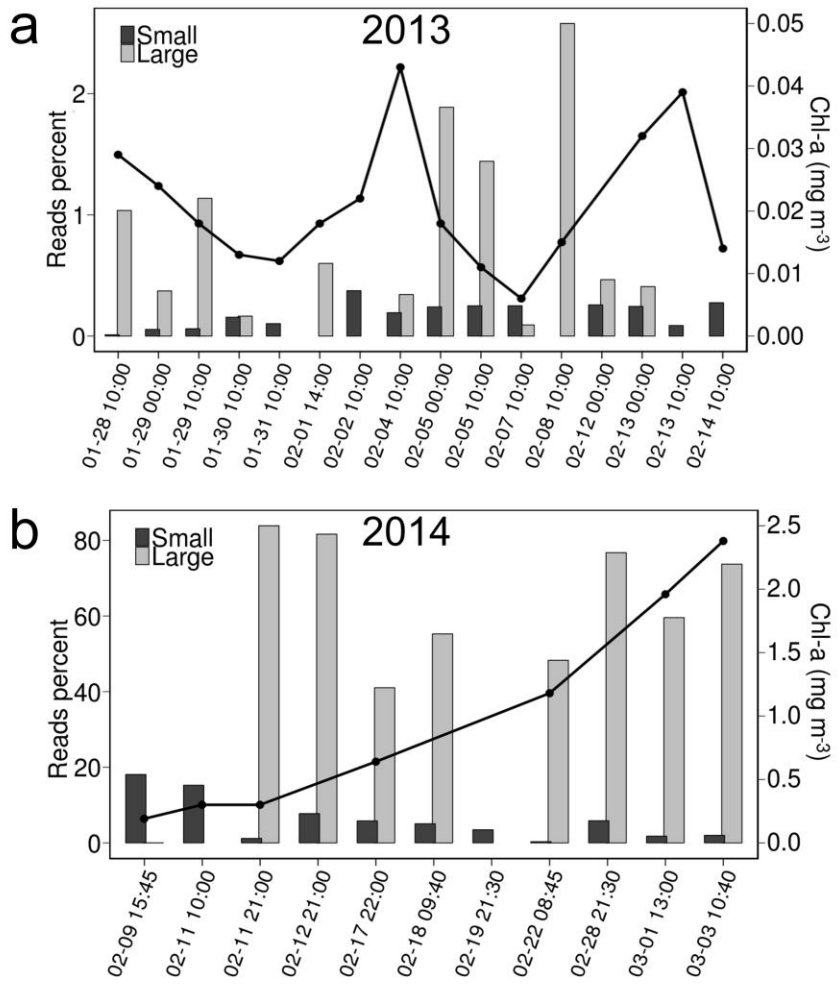
a
2013
Small
Large
Reads percent
Chl-a (mg m-3)
0
1
2
0.00
0.01
0.02
0.03
0.04
0.05
01-28 10:00
01-29 00:00
01-29 10:00
01-30 10:00
01-31 10:00
02-01 14:00
02-02 10:00
02-04 10:00
02-05 00:00
02-05 10:00
02-07 10:00
02-08 10:00
02-12 00:00
02-13 00:00
02-13 10:00
02-14 10:00
b
2014
Small
Large
Reads percent
Chl-a (mg m-3)
0
20
40
60
80
0.0
0.5
1.0
1.5
2.0
2.5
02-09 15:45
02-11 10:00
02-11 21:00
02-12 21:00
02-17 22:00
02-18 09:40
02-19 21:30
02-22 08:45
02-28 21:30
03-01 13:00
03-03 10:40

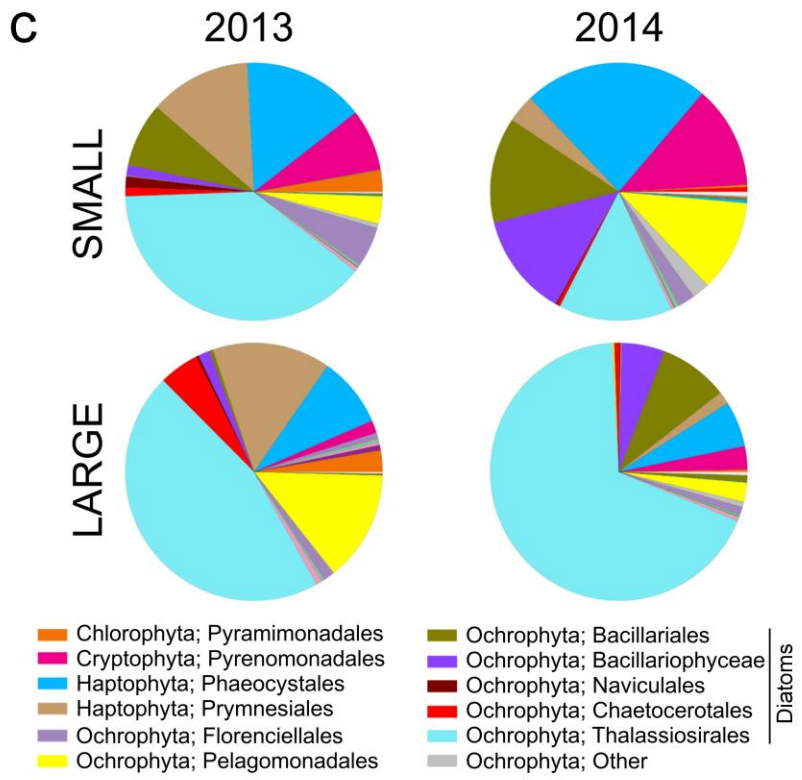
c
2013
2014
SMALL
LARGE
Chlorophyta; Pyramimonadales
Cryptophyta; Pyrenomonadales
Haptophyta; Phaeocystales
Haptophyta; Prymnesiales
Ochrophyta; Florenciellales
Ochrophyta; Pelagomonadales
Ochrophyta; Bacillariales
Ochrophyta; Bacillariophyceae
Ochrophyta; Naviculales
Ochrophyta; Chaetocerotales
Ochrophyta; Thalassiosirales
Ochrophyta; Other
Diatoms

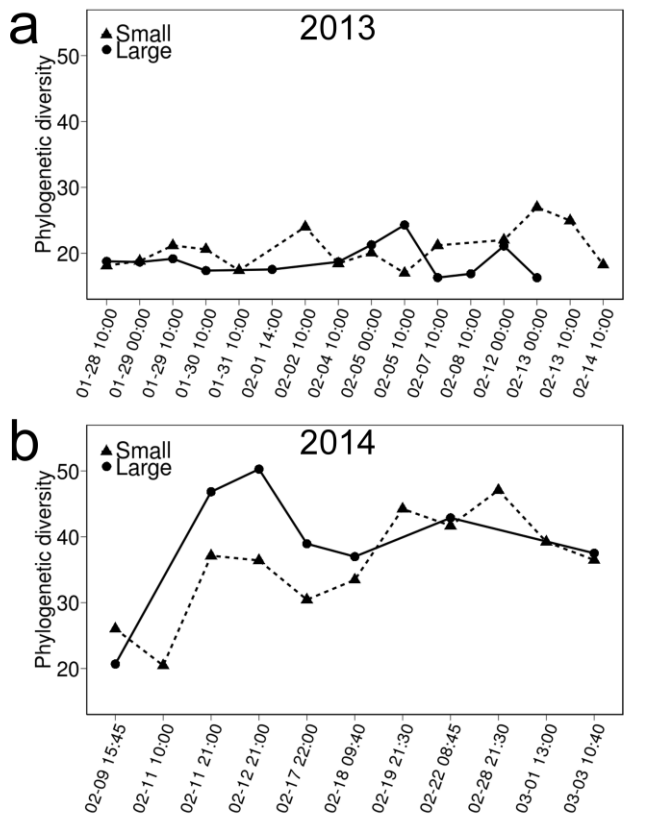
a
2013
Small
Large
Phylogenetic diversity
20
30
40
50
01-28 10:00
01-29 00:00
01-29 10:00
01-30 10:00
01-31 10:00
02-01 14:00
02-02 10:00
02-04 10:00
02-05 00:00
02-05 10:00
02-07 10:00
02-08 10:00
02-12 00:00
02-13 00:00
02-13 10:00
02-14 10:00
b
2014
Small
Large
Phylogenetic diversity
20
30
40
50
02-09 15:45
02-11 10:00
02-11 21:00
02-12 21:00
02-17 22:00
02-18 09:40
02-19 21:30
02-22 08:45
02-28 21:30
03-01 13:00
03-03 10:40

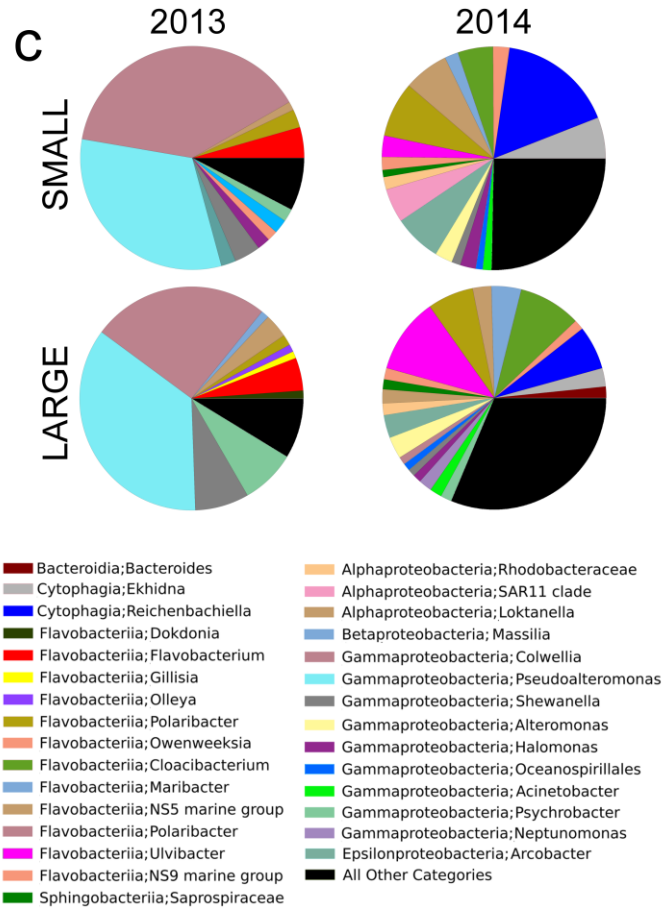
c
2013
2014
SMALL
LARGE
Bacteroidia;Bacteroides
Cytophagia;Ekhidna
Cytophagia;Reichenbachiella
Flavobacteriia;Dokdonia
Flavobacteriia;Flavobacterium
Flavobacteriia;Gillisia
Flavobacteriia;Olleya
Flavobacteriia;Polaribacter
Flavobacteriia;Owenweeksia
Flavobacteriia;Cloacibacterium
Flavobacteriia;Maribacter
Flavobacteriia;NS5 marine group
Flavobacteriia;Polaribacter
Flavobacteriia;Ulvibacter
Flavobacteriia;NS9 marine group
Sphingobacteriia;Saprospiraceae
Alphaproteobacteria;Rhodobacteraceae
Alphaproteobacteria;SAR11 clade
Alphaproteobacteria;Loktanella
Betaproteobacteria;Massilia
Gammaproteobacteria;Colwellia
Gammaproteobacteria;Pseudoalteromonas
Gammaproteobacteria;Shewanella
Gammaproteobacteria;Alteromonas
Gammaproteobacteria;Halomonas
Gammaproteobacteria;Oceanospirillales
Gammaproteobacteria;Acinetobacter
Gammaproteobacteria;Psychrobacter
Gammaproteobacteria;Neptunomonas
Epsilonproteobacteria;Arcobacter
All Other Categories

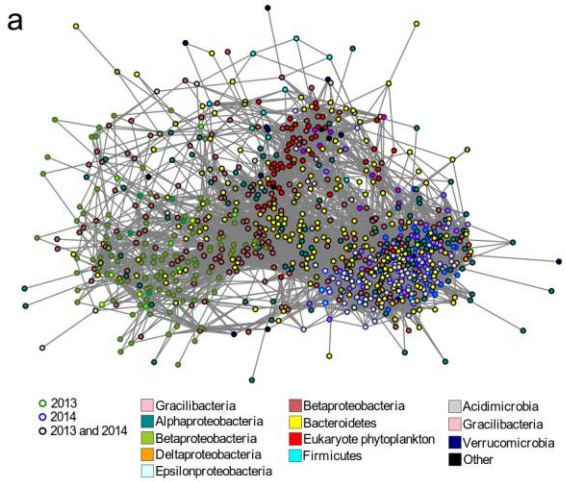

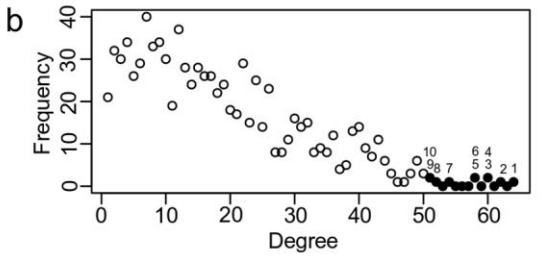

1. Neptunomonas, Gammaproteobacteria (1680561)
2. Reichenbachiella, Bacteroidetes (310713)
3. Ekhidna, Bacteroidetes (New.ReferenceOTU138)
4. Lutimonas, Flavobacteria (591430)
5. Reichenbachiella, Bacteroidetes (155856)
6. Alteromonas, Gammaproteobacteria (823476)
7. Arcobacter, Epsilonproteobacteria (810850)
8. Pseudophaeobacter, Alphaproteobacteria (575317)
9. Acinetobacter, Gammaproteobacteria (562618)
10. Rhodobacteraceae, Alphaproteobacteria (226155)